Available online at www.sciencedirect.com
SCIENCE DIRECT®
Bioorganic Chemistry 33 (2005) 484–492
BIOORGANIC CHEMISTRY
www.elsevier.com/locate/bioorg

DFT–GIAO study of aryltetralin lignan lactones: Conformational analyses and chemical shifts calculations

Jordi Casanovas [a,*], Adriana M. Namba [b],
R. da Silva [c], Carlos Alemán [d,*]

[a] *Departament de Química, Escola Politècnica Superior, Universitat de Lleida, c/Jaume II n^{o} 69, Lleida E-25001, Spain*
[b] *Departamento de Química, F.F.C.L.R.P., Universidade de São Paulo, Av. Bandeirantes, 3900, 14040-901, Ribeirão Preto - SP, Brazil*
[c] *Núcleo de Pesquisa em Ciencias Exatas e Tecnológicas da Universidade de Franca, Av. Dr. Armando Salles de Oliveira, 201, 14404-600, Franca, SP, Brazil*
[d] *Departament d'Enginyeria Química, ETSEIB, Universitat Politècnica de Catalunya, Diagonal 647, Barcelona E-08028, Spain*

Received 7 July 2005
Available online 11 November 2005

Abstract

The conformational properties of polygamain and morelensin, two aryltetralin lignan lactones, have been investigated in both the gas-phase and chloroform solution using DFT calculations at the B3LYP/6-311G(d,p) level. Results indicate that the conformation of polygamain is very rigid. Thus, the conformational flexibility of its five-membered rings is considerably restricted as reflects the pseudo-rotational parameters of the corresponding envelope conformations. On the other hand, morelensin shows a notable conformational flexibility, which is mainly due to its two methoxy groups. Accordingly, 16 minimum energy conformations with relative energies smaller than 2.4 kcal/mol were detected. Furthermore, chemical shifts for ^{13}C nuclei have been calculated using the GIAO method, results being compared with experimental data. A good agreement was found for both polygamain and morelensin.

Keywords: Lignans; Aryltetralin; Lactone; Polygamain; Morelensin; Conformational analyses; DFT calculations; GIAO calculations

---

[*] Corresponding authors.
E-mail addresses: jcasanovas@quimica.udl.es (J. Casanovas), carlos.aleman@upc.edu (C. Alemán).

0045-2068/$ - see front matter
doi:10.1016/j.bioorg.2005.10.003

1. Introduction

The ability to understand the conformational properties of complex bioorganic molecules is very useful in a range of chemical design applications including drug discovery and the design of targeted chemical hosts [1–4]. Many drugs-like compounds possess flexible cyclic and acyclic moieties that induce the apparition of minimum energy conformations very close in energy, i.e., the potential energy hypersurface (PEHS) is very flat. The application of sophisticated theoretical methods to explore the PEHS of these compounds is a problem of considerable interest. However, this complex task requires huge amounts of computational resources if reliable results want to be achieved.

In a recent study, da Silva et al. [5] reported a complete and accurate NMR analysis of several aryltetralin lignan lactones, which is expected to make easier the stereochemical determination of new analogues. Lignans are a large family of natural products widely distributed in the plant kingdom. Among them, aryltetralin lignan lactones have shown to possess antiviral- and antitumor-promoting activities [6–9]. As a consequence of these biological properties, the chemistry of aryltetralin lignan lactones is receiving much attention. In spite of the fact that the results of da Silva et al. [5] have enlarged the NMR database of aryltetralin lignan lactones, which was considerably scarce at that moment [10–13], no information about the conformational preferences was derived from such study.

In this work, we present a density functional theory (DFT) study about the conformational properties of polygamain (**1**) and morelensin (**2**), the chemical structure of these aryltetralin lignan lactones being displayed in Fig. 1. More specifically, detailed conformational searches have been performed to identify and characterize their minimum energy conformations in both gas-phase and chloroform solution. To confirm the reliability of the results, chemical shifts have been calculated and compared with the available experimental information [5]. Calculations reveal that **1** is a stiff molecule, while the high conformational flexibility of **2** mainly resides on the two methoxy groups.

2. Methods

Geometry optimizations were performed in the gas-phase using the B3LYP hybrid functional [14,15] combined with the 6-311G(d,p) basis set [16]. To explore systematically their conformational preferences, all the degrees of freedom of **1** and **2** have been considered. It should be noted that the five-membered ring fused with the cyclohexane, denoted ring ***A*** in Fig. 1, is severely restricted to a C_{12}-*endo* envelope conformation by the sp^2 hybridization of C_1 and the stereochemistry of C_{12} and C_2. Furthermore, the conformation of the cyclohexane ring is also restricted by its two adjacent fused rings. Accordingly, the degrees of freedom expected for **1** and **2** are: (a) two five-membered rings, denoted rings ***B*** and ***C*** in Fig. 1; (b) the torsional angle around the inter-ring bond C_3–$C_{1'}$, denoted χ (Fig. 1); and (c) the torsional angles around the $C_{3'}$–O and $C_{4'}$–O bonds of **2**, denoted ξ_1 and ξ_2 (Fig. 1), respectively. The following minima are expected for these degrees of freedom: (a) C_7-*exo* ↔ C_7-*endo* and $C_{7'}$-*exo* ↔ $C_{7'}$-*endo* for rings ***B*** and ***C***, respectively; and (b) *gauche*$^+$, *trans*, and *gauche*$^-$ rotamers for each of the three torsional angles χ, ξ_1, and ξ_2. Accordingly, $2(\boldsymbol{B}) \times 2(\boldsymbol{C}) \times 3(\chi) = 12$ starting geometries were considered for the conformational study of **1**. The minimum energy conformations found for **1** (N) were considered as good starting points for the conformational study of **2**, which were combined with the

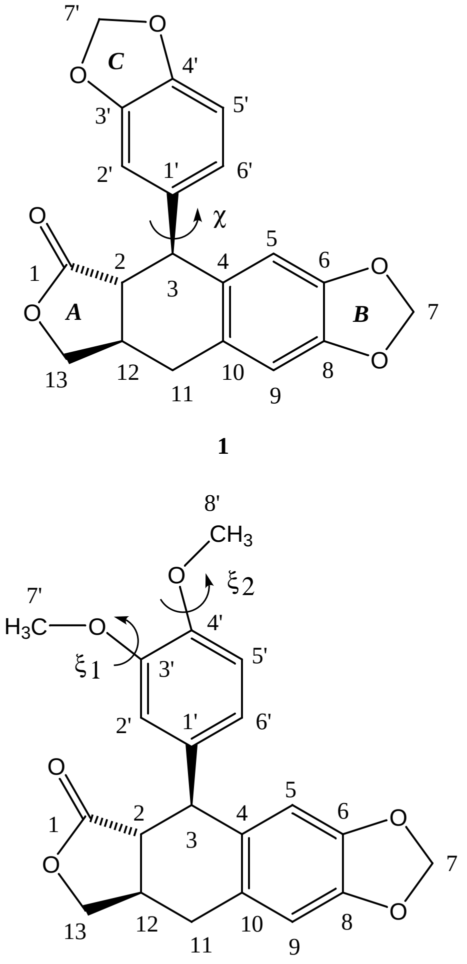

1

2

Fig. 1. Chemical structure of polygamain (**1**) and morelensin (**2**). Atom numbering and labels for both five-membered rings and dihedral angles are indicated.

minima expected for the torsional angles ξ_1 and ξ_2. Thus, $N \times 3(\xi_1) \times 3(\xi_1)$ structures were used as starting point in geometry optimizations of **2**.

To obtain an estimation of the solvation effects, single point calculations were also conducted on the gas-phase optimized geometries using a Self-Consistent Reaction-Field (SCRF) model. SCRF methods treat the solute at the quantum mechanical level, while the solvent is represented as a dielectric continuum. Specifically, we chose the Polarizable Continuum Model (PCM) developed by Tomasi and co-workers to describe the bulk solvent [17,18]. The PCM represents the polarization of the liquid by a charge density appearing on the surface of the cavity created in the solvent, i.e., the solute/solvent interface. This cavity is built using a molecular shape algorithm. PCM calculations were performed in the framework of the B3LYP/6-311G(d,p) level using the standard protocol and considering the dielectric constant of chloroform ($\varepsilon = 4.9$). The conformational free energies in solution ($\Delta\Delta G_{\text{conf}}$) were estimated using the classical thermodynamical scheme: the free energies of solvation (ΔG_{sol}) provided by the PCM model were added to conformational energies in the gas-phase.

Carbon isotropic shielding constants were computed at the B3LYP/6-311G(d) level using perturbation theory and the Gauche Invariant Atomic Orbitals (GIAO) method [19,20]. Theoretical calculations yield absolute values of the isotropic shielding constant (σ) with respect to the bare nucleus in vacuo whereas experimental data are referred to an usual standard as TMS. Thus, experimental scale δ (chemical shift) is related to the theoretical scale σ via

$$\delta = \sigma - \sigma_o, \tag{1}$$

where σ_o is the theoretical value of the reference. The ^{13}C isotropic shielding constants in TMS were computed in a previous work at the level of theory used in this study [21].

The statistical evaluation of the similarity between experimental and calculated chemical shifts was carried out considering the scaling coefficient (c) and the correlation coefficient (r) for a regression of the type $y = c \cdot x$ and the root-mean-square deviation (rms).

3. Results and discussion

3.1. Polygamain (*1*)

Geometry optimization of the 12 structures generated and used as starting points led to only four different minimum energy conformations. Table 1 shows the more relevant conformational features and the relative energies (ΔE) of these structures. Interestingly, the four structures share a common conformational feature: the dihedral angle χ is about ~133°. Thus, these spatial arrangements allow minimize the repulsive interactions between the carbonyl group of ***A*** and the six-membered ring fused to ***C***. As can be seen, the four minima only differ in the conformation of rings ***B*** and ***C***, which is C$_7$-*endo* and C$_{7'}$-*exo*, respectively, for the lowest energy conformation **1a** (Fig. 2). The **1b**, **1c**, and **1d** conformations are only 0.2 or 0.3 kcal/mol less favored than **1a** indicating that the two envelope conformations of rings ***B*** and ***C*** are very close in energy.

Another point that deserves special attention is the difference in the amplitude (τ_m) and phase angle (P) of the envelope forms found for five-membered rings ***A***, ***B***, and ***C***, such differences being detected in the four minima listed in Table 1. Thus, the values of such pseudorotational parameters, which were calculated according to Altona and Sundaralingam [22,23] are: ring ***A*** [$P \approx 12.5°$, $\tau_m \approx 38.2°$], ring ***B*** [$P \approx 90.5°/-88.8°$ (C$_7$-*exo*/C$_7$-*endo*),

Table 1
Minimum energy conformations of polygamain[a] (**1**)

Minimum	Ring ***B***	Ring ***C***	χ	ΔE[b]	ΔG_{sol}[b]	$\Delta\Delta G_{\text{conf}}$[b]
1a	C$_7$-*endo*	C$_{7'}$-*exo*	133.5	0.0[c]	−4.6	0.0
1b	C$_7$-*exo*	C$_{7'}$-*exo*	133.0	0.2	−4.7	0.2
1c	C$_7$-*endo*	C$_{7'}$-*endo*	133.1	0.2	−4.7	0.1
1d	C$_7$-*exo*	C$_{7'}$-*endo*	134.2	0.3	−4.8	0.2

[a] See Fig. 1.

[b] In kilocalorie per mole.

[c] $E = -1223.373371$ a.u.

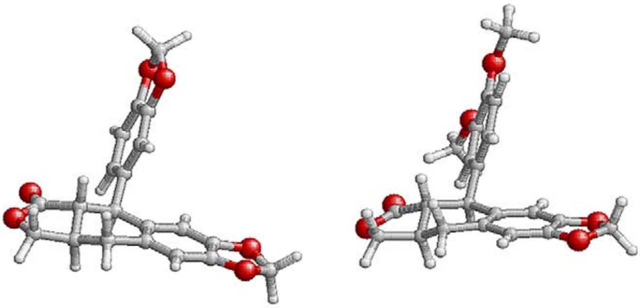

1a **2a**

Fig. 2. B3LYP/6-311G(d,p) lowest energy structures of polygamain (**1a**) and morelensin (**2a**).

$\tau_m \approx 14.3°$] and ring ***C*** [$P \approx +90.6°/-89.7°$ ($C_{7'}$-*exo*/$C_{7'}$-*endo*), $\tau_m \approx 13.1°$]. As can be seen, the value of τ_m determined for ring ***A*** agrees with those typically found for the envelope conformations of non-fused five-membered ring compounds [23–26]. However, the amplitudes calculated for rings ***B*** and ***C*** are very small indicating that their envelope conformations are close to planarity, which is in agreement with the small relative energies listed in Table 1. The differences between the envelope conformations of the three rings are illustrated for minimum **1a** in Fig. 2.

These small conformational differences are also responsible for the similarities between the ΔG_{sol} values computed in chloroform solution (Table 1), the largest difference being 0.2 kcal/mol. The $\Delta\Delta G_{conf}$ values, which are included in Table 1, show that the influence of the solvent in the conformational equilibrium associated to the minima of **1** is very small. The overall of these results indicates that, in spite of its degrees of freedom, the structure of **1** is considerably stiff. Thus, the flexible inter-ring torsional angle χ is severely restricted by steric repulsions, and the amplitude of the envelope conformations found for rings ***B*** and ***C*** is very small. Consequently, the differences between minima **1a**–**1d** are very small in terms of both geometries and energies.

As expected NMR chemical shifts calculated for the four minima were very similar among them, the largest difference being 0.7 ppm. In spite of this similitude, calculated chemical shifts were averaged assuming a Boltzmann distribution of the four minima, which was calculated using the $\Delta\Delta G_{conf}$ values displayed in Table 1. The theoretical and experimental values of δ (^{13}C) are listed in Table 2, while the statistical results derived from the comparison between them are displayed in Table 3.

As is reflected by the coefficients *r*, the correlation between the experimental chemical shifts and those predicted for **1** is very good. Thus, the scaling coefficient indicates that the predicted δ (^{13}C) are overestimated by 5%. This error and the rms value listed in Table 3, are within the range typically found in the literature [27–29].

3.2. Morelensin (2)

As can be seen in Fig. 1, compound **2** differs from **1** in the ring ***C***, which is replaced by two methoxy groups. Accordingly, **1a** and **1b** are the only suitable minimum energy conformations of **1** to generate the starting structures for geometry optimization of **2**, i.e., **1c** and **1d** differ from **1a** and **1b** in the arrangement of ***C***. Thus, considering $N = 2$ (see Section 2), $2(N) \times 3(\xi_1) \times 3(\xi_2) = 18$ initial structures were used for the conformational search of **2**.

Table 2
Calculated and experimental ^{13}C chemical shifts[a] for polygamain[b] (**1**) and morelensin[b] (**2**)

	1			**2**	
	$\delta_{\text{calculated}}$	$\delta_{\text{experimental}}$		$\delta_{\text{calculated}}$	$\delta_{\text{experimental}}$
C1′	146.1	135.9	C1′	145.0	134.6
C2′	116.3	107.5	C2′	123.2	110.5
C3′	153.7	146.8	C3′	156.4	146.5
C4′	153.0	145.7	C4′	156.9	146.5
C5′	111.5	107.2	C5′	114.4	111.3
C6′	127.1	122.1	C6′	123.9	121.6
C7′	106.4	100.0	C7′	56.7	56.5
			C8′	55.7	56.0
C1	178.7	174.5	C1	179.7	174.5
C2	54.3	47.8	C2	54.8	47.6
C3	52.5	45.1	C3	51.6	45.3
C4	142.2	131.7	C4	142.1	132.0
C5	115.5	109.0	C5	115.9	108.2
C6	153.5	145.5	C6	153.4	145.7
C7	106.8	100.1	C7	106.7	100.2
C8	153.1	145.5	C8	153.0	146.3
C9	111.6	108.1	C9	111.5	107.3
C10	135.5	126.8	C10	135.9	127.0
C11	37.5	32.5	C11	37.5	32.3
C12	45.3	39.0	C12	45.6	39.4
C13	73.3	70.0	C13	73.4	70.7

[a] In ppm. Experimental data from [5].

[b] See Fig. 1.

Table 3
Statistical results[a] derived from the comparison between the calculated and experimental ^{13}C chemical shifts in polygamain (**1**) and morelensin (**2**)

Compound	*c*	*r*	rms
1	0.95	0.996	6.94
2	0.94	0.995	7.19

[a] Scaling coefficient (c) and correlation coefficient (r) from $y = c \cdot x$, and root-mean-square deviation (rms; in ppm).

Table 4 provides the more important conformational characteristics and the ΔE values of the minimum energy conformations resulting from B3LYP/6-311G(d,p) geometry optimizations in the gas-phase. The methoxy groups impart a considerable degree of flexibility to the compound, as is reflected by the 16 minima found. As can be seen, for every arrangement of the side chains, which is specified by ξ_1 and ξ_2, two minima that only differ in the envelope conformation of ***B*** can be identified. In all cases, the amplitude and phase angle of rings ***A*** and ***B*** were similar to those described for **1**. To minimize the steric repulsions between the methoxy groups and ***A***, the inter-ring dihedral angle χ is restricted to values ranging from 130° to 146°.

In the lowest energy structure **2a**, which is displayed in Fig. 2, the two methoxy groups are arranged in *trans* and ***B*** adopts a C_7-*endo* conformation. Minimum **2b** is destabilized by only 0.2 kcal/mol since it differs from **2a** in the conformation of the five-membered ring

Table 4
Minimum energy conformations of morelensin[a] (**2**)

Minimum	Ring B	χ	ξ_1	ξ_2	ΔE[b]	ΔG_{sol}[b]	$\Delta\Delta G_{conf}$[b]
2a	C_7-*endo*	144.4	−176.6	179.8	0.0[c]	−2.7	0.1
2b	C_7-*exo*	144.5	−176.6	180.0	0.2	−3.0	0.0
2c	C_7-*endo*	145.6	−174.1	−65.4	0.6	−2.0	1.4
2d	C_7-*exo*	145.5	−174.1	−65.6	0.6	−1.9	1.5
2e	C_7-*endo*	132.9	−72.1	178.0	1.1	−3.1	0.8
2f	C_7-*exo*	132.9	−72.2	180.0	1.2	−3.2	0.8
2g	C_7-*endo*	134.0	105.3	−69.1	1.7	−2.1	2.4
2h	C_7-*exo*	134.1	105.3	−69.1	1.7	−2.1	2.4
2i	C_7-*endo*	134.0	−75.7	−69.2	1.7	−2.1	2.4
2j	C_7-*exo*	134.0	−75.8	−69.1	1.8	−1.9	2.7
2k	C_7-*endo*	132.4	68.2	176.7	1.8	−3.6	1.0
2l	C_7-*exo*	131.2	68.4	175.1	2.1	−3.5	1.4
2m	C_7-*exo*	130.2	−111.5	70.0	2.2	−2.5	2.5
2n	C_7-*endo*	130.3	−111.5	70.1	2.2	−2.6	2.4
2o	C_7-*endo*	130.3	70.6	70.1	2.2	−2.6	2.4
2p	C_7-*exo*	130.6	70.6	70.1	2.3	−2.8	2.3

[a] See Fig. 1.
[b] In kilocalorie per mole.
[c] $E = -1263.899394$ a.u.

B but not in ξ_1 and ξ_2. On the other hand, **2c**, **2d**, **2e** and **2f** differ from **2a** and **2b** in either ξ_1 or ξ_2, which changes from *trans* to *gauche*$^-$. The ΔE values of **2c** and **2d** are 0.6 kcal/mol, this destabilization being fully consistent with the values reported in the literature for the rotation of a single C–O bond [30,31]. However, the ΔE calculated for **2e** and **2f** is 1.1 and 1.2 kcal/mol, respectively, indicating that the unfavorable interactions between (i) the methoxy group attached to $C_{3'}$ and ***A*** and (ii) the disadvantageous rotation of the dimethoxyaryl group each amount to 0.5–0.6 kcal/mol. The remaining minima are not significant in the gas-phase since their population is expected to be negligible, i.e., ΔE values are higher than 1.5 kcal/mol.

Solvent effects produce some changes in the relative energy order between the different conformers. The more favored conformations in chloroform solution are **2a** and **2b**, which are almost isoenergetic, as in the gas-phase. However, **2c** and **2d** become about 0.8 kcal/mol less stable in solution than in the gas-phase, while **2e** and **2f** are stabilized by about 0.4 kcal/mol, their ΔE values being very similar. Furthermore, the interactions with the solvent stabilize **2k** and **2l** by 0.6 and 0.5 kcal/mol with respect to **2b**. The overall of these changes indicates that solvent not only alters the populations of the different minima but also increases the number of significant minima from 6 to 8.

The theoretical values of δ (^{13}C) were calculated for all the minimum energy conformations listed in Table 4. Theoretical values averaged according to a Boltzmann distribution of the minima in solution are compared with experimental data in Table 2, the statistical parameters of such comparison being included in Table 3. The statistical parameters obtained for δ (^{13}C) are very similar to those obtained for **1**, the rms being of 1.11 ppm. Thus, although quantum mechanical calculations overestimate the δ (^{13}C) values, experimental data are in general well reproduced by the conformational model displayed in Table 4.

4. Conclusions

The results presented in this work indicate that **1** adopts a rigid structure, the only degrees of freedom being the rings ***B*** and ***C*** that can adopt C_7-*exo*/C_7-*endo* and $C_{7'}$-*exo*/$C_{7'}$-*endo* envelope conformations, respectively. Furthermore these conformations could be considered as distorted planar arrangements, as reveal the small pseudorotational amplitudes. Regarding **2**, the methoxy groups attached to $C_{3'}$ and $C_{4'}$ provide a notable conformational flexibility that combines with the C_7-*exo*/C_7-*endo* envelope conformations of ***B***. The chemical shifts predicted for the conformational models proposed for **1** and **2** are in good agreement with the reported experimental data.

Acknowledgments

Authors are indebted to the "Centre de Supercomputació de Catalunya" (CESCA) and "Centre Europeu de Paral·lelisme de Barcelona" (CEPBA) for computational facilities. A.M.N. wishes to thank the Fundação de Amparo à Pesquisa do Estado de São Paulo (FAPESP).

References

[1] S. Putta, G.A. Landrum, J.E. Penzotti, J. Med. Chem. 48 (2005) 3313–3318.
[2] N. Moitessier, C. Henry, B. Maigret, Y. Chapleur, J. Med. Chem. 47 (2004) 4178–4187.
[3] S. Handschuh, J. Gasteiger, J. Mol. Model. 6 (2000) 358–378.
[4] C.A. Parish, M. Yarger, K. Sinclair, K. Dure, A. Goldberg, J. Med. Chem. 47 (2004) 4838–4850.
[5] R. da Silva, V.C.G. Heleno, S. de Albuquerque, J.K. Bastos, M.L. Andrade e Silva, P.M. Donate, G.V.J. da Silva, Magn. Reson. Chem. 42 (2004) 985–989.
[6] D. Ayres, J.D. Loike, Lignans. Chemical, Biological and Clinical Properties, Cambridge University Press, Cambridge, 1990.
[7] E. Eich, H. Pertz, M. Kaloga, J. Schultz, M.R. Fesen, A. Mazumder, Y. Pommier, J. Med. Chem. 39 (1996) 86–95.
[8] C. Ito, M. Itoigawa, M. Ogata, X.Y. Mou, H. Tokuda, H. Nishino, H. Furukawa, Plant. Med. 67 (2001) 166–168.
[9] M.A. Castro, J.M. Miguel del Corral, M. Gordaliza, M.A. Gómez-Zurita, P.A. García, A. San Feliciano, Phytochem. Rev. 2 (2003) 219–228.
[10] L. Udino, J. Abaul, P. Bourgeous, L. Gorrichon, H. Duran, C. Zedde, Planta Med. 65 (1999) 279–281.
[11] G. Matthee, A.D. Wright, G.M. König, Plant. Med. 65 (1999) 493.
[12] W.H. Lin, J.M. Fang, Y.S. Cheng, Phytochemistry 50 (1999) 653–658.
[13] E.E.D.A. Blumenthal, M.S. da Silva, M. Yoshida, Phytochemistry 46 (1997) 745–749.
[14] A.D. Becke, J. Chem. Phys. 98 (1993) 5648–5652.
[15] C.T. Lee, W.T. Yang, R.G. Parr, Phys. Rev. B 37 (1988) 785–789.
[16] P.C. Hariharan, J.A. Pople, Chem. Phys. Lett. 16 (1972) 217–222.
[17] M. Miertus, E. Scrocco, J. Tomasi, Chem. Phys. 55 (1981) 117–129.
[18] S. Miertus, J. Tomasi, Chem. Phys. 65 (1982) 239–252.
[19] R. Ditchfield, J. Chem. Phys. 56 (1972) 5688–5692.
[20] P. Pulay, K. Wolinski, J.F. Hinton, J. Am. Chem. Soc. 112 (1990) 8251–8260.
[21] J. Casanovas, J. Pacchioni, F. Illas, Mater. Sci. Eng. B 68 (1999) 16–21.
[22] C. Altona, M. Sundaralingam, J. Am. Chem. Soc. 94 (1972) 8205–8212.
[23] C. Altona, M. Sundaralingam, J. Am. Chem. Soc. 95 (1973) 2333–2344.
[24] J. Plavec, W. Tong, J. Chattopadhyaya, J. Am. Chem. Soc. 115 (1993) 9734–9746.
[25] K.A. Brameld, W.A. Goddard III, J. Am. Chem. Soc. 121 (1999) 985–993.
[26] C. Alemán, A. Martín ez de Ilarduya, E. Giralt, S. Muñoz-Guerra, Tetrahedron 52 (1996) 8275–8286.
[27] T. Helgaker, M. Jaszunski, K. Ruud, Chem. Rev. 99 (1999) 293–352.

[28] M. Bühl, M. Kaupp, O.L. Malkina, V.G. Malkin, J. Comput. Chem. 20 (1999) 91–105.
[29] D.D. Laws, H. Le, A.C. de Dios, R.H. Havlin, E. Oldfield, J. Am. Chem. Soc. 117 (1995) 9542–9546.
[30] A.M. Namba, S. León, G.V.J. da Silva, C. Alemán, J. Comput. Aided Mol. Des. 15 (2001) 235–245.
[31] D.S. Maxwell, J. Tirado-Rives, W.L. Jorgensen, J. Comput. Chem. 16 (1995) 984–1010.